Published in final edited form as:
Cell Calcium. 2011 March ; 49(3): 162–173. doi:10.1016/j.ceca.2011.01.008.

Regulation of Cardiac Ca^{2+} Channel by Extracellular Na^{+}

Shahrzad Movafagh[1], **Lars Cleemann**[2], and **Martin Morad**[1,2]

[1] Department of Pharmacology, Georgetown University Medical Center, Washington, DC 20007 USA

[2] Cardiac Signaling Center of University of South Carolina, Medical University of South Carolina & Clemson University, Charleston, SC 29425 USA

Abstract

Hyponatremia is a predictor of poor cardiovascular outcomes during acute myocardial infarction and in the setting of preexisting heart failure [1]. There are no definitive mechanisms as to how hyponatremia suppresses cardiac function. In this report we provide evidence for direct down-regulation of Ca^{2+} channel current in response to low serum Na^{+}. In voltage-clamped rat ventricular myocytes or HEK 293 cells expressing the L-type Ca^{2+} channel, a 15 mM drop in extracellular Na^{+} suppressed the Ca^{2+} current by ~15%; with maximal suppression of ~30% when Na^{+} levels were reduced to 100 mM or less. The suppressive effects of low Na^{+} on I_{Ca}, in part, depended on the substituting monovalent species (Li^{+}, Cs^{+}, TEA^{+}), but were independent of phosphorylation state of the channel and possible influx of Ca^{2+} on Na^{+}/Ca^{2+} exchanger. Acidification sensitized the Ca^{2+} channel current to Na^{+} withdrawal. Collectively our data suggest that Na^{+} and H^{+} may interact with regulatory site(s) at the outer recesses of the Ca^{2+} channel pore thereby directly modulating the electro-diffusion of the permeating divalents (Ca^{2+}, Ba^{2+}).

Keywords

L-type Ca^{2+} channel; Na^{+}-regulation; cardiac myocytes; ion channels; PKA phosphorylation; Ca^{2+} channel agonists; Bay K 8644

1. Introduction

Voltage-gated L-type Ca^{2+} channels are essential regulators of a number of cardiac functions as they provide the critical trans-membrane influx of Ca^{2+} that triggers the release of Ca^{2+} from the sarcoplasmic reticulum (SR) for activation of contraction. L-type Ca^{2+} channels have been extensively studied in terms of their permeability, selectivity, gating, molecular structure and regulation. Despite high selectivity of these channels to Ca^{2+}, earlier studies reported significant permeability also to other divalents and monovalents, especially Na^{+} in absence of Ca^{2+} [2]. In addition, a number studies have shown suppression of I_{Ca} on withdrawal of Na^{+} in the presence of Ca^{2+} consistent, perhaps, with significant Na^{+} permeability of the Ca^{2+} channel [3–6]. This effect appeared to depend on the substituting

Corresponding Author: Martin Morad, MUSC, Cardiac Signaling Center, BSB 358, 173 Ashley Avenue, MSC 505, Charleston, SC 29425-5050, USA, Tel: (843) 792-3898, Fax: (843) 792-4606, moradm@musc.edu.

Disclosures: None declared

monovalent cations such that while replacement of Na^+ with Cs^+, TEA^+ and Li^+ reduced I_{Ca} significantly, substitution by TrisCl had little or no effect on I_{Ca} [7]. Studies substituting equi-osmolar sucrose or mannitol for NaCl were inconclusive as they destabilize the myocytes [8–11]. The two mechanisms proposed for low Na^+ suppressive effects on I_{Ca} were: 1) Inactivation of Ca^{2+} channels secondary to influx of Ca^{2+} on the Na^+/Ca^{2+} exchanger (NCX), on withdrawal of Na^+ [5]; and 2) Significant permeation of Na^+ through the channel in the presence of Ca^{2+}. The first mechanism appears to be unlikely as Na^+ removal continues to suppress the channel even when Ba^{2+} is the charge carrier [7,11]. The most compelling evidence against the second, direct Na^+ permeation, possibility was the finding that 1 μM of extracellular Ca^{2+} blocked the permeation of high concentrations of monovalents, consistent with high selectivity (>1/10,000) of the channel to Ca^{2+} [3,12–13].

More recent reports provide yet another possibility that positive or negative regulation of channel current by extracellular cations results from their binding and electrostatic interactions with specific pore-forming residues of the channel, as for instance described for the voltage-dependent blockade of Na^+ channels by Ca^{2+} [14], or electrostatic interactions of extracellular protons with glutamate residues of Ca^{2+} channels that mediate the suppressive effects of proton on I_{Ca} [15–16].

The aim of our study was to examine the low Na^+ suppressive effects on I_{Ca} in terms of direct interaction of Na^+ with the Ca^{2+} channel pore. We hypothesized that interaction of Na^+ within the channel pore, in the presence of Ca^{2+}, may increase the open probability of the channel, thus enhancing Ca^{2+} permeation of the channel. We have examined the effect of Na^+ withdrawal on whole cell I_{Ca} using both rat ventricular myocytes and HEK 293 cells expressing the recombinant L-type Ca^{2+} channel. In addition to reexamining the previous hypotheses regarding substituted monovalent species and possible influx of Ca^{2+} on NCX, we used several novel approaches that include: Quantifying the concentration- and voltage-dependent effects of Na^+ withdrawal on I_{Ca}; examining the efficacy of I_{Ca} suppression as the channel mean open-time was increased by (s)-(−) Bay K 8644, phosphorylation, or substituting Ba^{2+} for Ca^{2+} as the permeant divalent; and determining possible overlapping functions of Na^+ and H^+ at extracellular regulatory sites associated with the channel pore.

Our data support the possibility that extracellular Na^+ modulates the Ca^+ channel by displacing H^+ from a low affinity binding sites, in the electrostatically crowded environment of the channel pore.

2. Methods

2.1. Enzymatic isolation of Cardiac myocytes

Cardiac cells were isolated from adult male Wistar rats (200–300 g) through enzymatic digestion of cardiac tissue as described previously [17]. All animal experiments were conducted in accordance with Georgetown University Animal Care and Use Committee. Rats were anesthetized by *i.p.* injection of sodium pentobarbital (150 mg/kg) after which the heart was rapidly excised from the chest cavity and transferred to a Langendorff apparatus to undergo retrograde perfusion through the aorta at a rate of 7 ml/min. Initially, a Ca^{2+}-free Tyrode's solution (In mM: 137 NaCl, 5.4 K L-glutamate, 10 HEPES, 1 $MgCl_2$, 10 Glucose, pH 7.35 at 37 °C) was perfused for 6 min followed by the same Ca^{2+} free solution containing collagenase (1.4 mg/ml; Roche) and protease (0.16 mg/ml; Sigma-Aldrich) for 13 min and a final 6 min perfusion with the Tyrode's solution containing 0.2 mM $CaCl_2$. The right and left ventricles of the digested heart were then cut into several sections and single cells were isolated by gently agitating the tissue. Cells were stored on cover slips at room temperature in 0.2 mM $CaCl_2$ Tyrode's solution. Following a cell adhesion period (~ 30

min), the cover slips were transferred to the stage of an inverted Nikon microscope for patch-clamp experiments.

2.2. Transient Transfections

Recombinant Ca^{2+} channel subunits $\alpha_{1C,77}$-YFP, β_1, and $\alpha_2\delta$ were a generous contribution of Dr. Nikolai Soldatov (NIA, Baltimore MD). HEK 293 cells were grown in 6-well plates using Dulbecco's Modified Eagle Medium with 10% fetal bovine serum at 90% confluence. Using Lipofectamine™ 2000 (Invitrogen) gene transfection assay, 1–6 μg of each subunit was mixed with a standard amount of lipofectamine reagent and incubated for about 20 minutes. After incubation, the mixture was transferred to each well while swirling the plates. Cells were then incubated for 24 hours allowing for gene expression to take place. The next day, cells were split onto cover slips at 10% confluence and allowed to incubate for another 48 hours before being used for patch-clamp studies. Gene expression was determined at a rate of 60–70% using a GFP fluorescence filter (Chroma Technology) for excitation/emission at 470/525 nm. The GFP-filter cube was inserted into the epi-fluorescence light pass of the Nikon Diaphot inverted microscope and illuminated by a RatioArc mercury lamp. Cells expressing green fluorescence were used for patch-clamp experiments.

2.3. Electrophysiology

Ca^{2+} current (I_{Ca}) measurements—Patch pipettes (2–5 MΩ) were filled with an internal solution containing (mM): 120 CsOH, 110 aspartic acid, 20 TEACl, 2 EGTA, 5 MgATP, 20 HEPES, titrated to pH 7.2. In some experiments 200 μM cAMP was added to the pipette solution to fully activate PKA phosphorylation. Cells were voltage-clamped at a holding potential of −50 mV to inactivate Na^+ channels. Peak I_{Ca} was measured using 25–50 ms depolarization pulses to 0 or 10 mV. For current-voltage (I-V) relationships we used test potentials ranging from −40 to +80 mV with 10 mV increments. Steady-state availability was measured by varying a 500 ms preconditioning potential from −80 mV to +30 mV, followed by a test pulse to +10 mV. Activation plots were measured by normalizing I-V currents to peak value at ~0 mV for each cell before and after solution exchange. Activation and availability plots were individually fitted using a standard Boltzmann function:

$$f(v)=\frac{I_{max}}{1+e^{(v_{0.5}-v)/v_c}}+c$$

where $V_{0.5}$ and the slope factor, V_c, were obtained using Origin6.0 software. All records were bracketed before and after solutions exchange to obtain individual baseline values for each cell. Currents were recorded using a Dagan amplifier and pClamp 5.5 software (Axon Instruments). Data were analyzed and plotted using Origin6.0 and pClamp 9.0 software. Currents were paired with baseline values before each intervention and the means were compared using a paired Student's t-test. ANOVA was used to compare group means. Results are shown as mean ± S.E.

2.4. Chemicals and Solutions

The standard extracellular Tyrode's solution contained (mM): 145 NaCl, 1 $MgCl_2$, 10 HEPES, 10 glucose, and 2 $CaCl_2$. pH was titrated to 7.4 using NaOH. KCl was removed from external solutions to prevent I_K activation. Reduced values of $[Na^+]_o$ in the range from 130–5 mM were achieved by replacement of NaCl with equimolar concentrations of, CsCl, TEACl, or LiCl or equiosmolar concentrations of sucrose. In order to inhibit Na^+/Ca^+ exchanger from operating in the Ca^{2+}-influx (reverse) mode under low $[Na^+]$ experiments, NaCl was removed from internal solutions. In addition, in some experiments we used 1–5

μM of tetrodotoxin (TTX; Alamone Laboratories) to block voltage-gated Na^+ channels. (S)-(−)-Bay K 8644 was obtained from Sigma-Aldrich Inc. (St. Louis, MO). To characterize membrane responses we used a rapid solution exchange system well established in our laboratory and previously described [18]. In short, solutions were placed in a five barrel apparatus attached to electronically operated valves that connected through 5 separate manifolds into a single outflow tip located ~0.2 mm from the cell. Upon commanding the electronic unit, solution was discharged from the tip within 20 ms. Complete superfusion was achieved in ~50 ms. All experiments were carried out at room temperature.

3. Results

3.1. Exploring the effect of extracellular [Na^+] on I_{Ca}

To examine the regulatory role of extracellular Na^+ on ventricular L-type Ca^{2+} current, we reduced the extracellular [Na^+] to10 mM from its control value of 145 mM, by replacing it with equimolar concentrations of Cs^+. Figure 1 shows the effect of rapid (50 ms) reduction of external [Na^+] to 10 mM on I_{Ca} activated by step depolarizations from −50 to 0 mV for 100 ms. In some experiments, in addition to a holding potential of −50 mV, 5–10 μM of TTX was required to fully suppress I_{Na}. Figure 1A shows that I_{Ca} decreased by 35 % within first three depolarizing pulses (representative currents, panel C) applied at 5 sec intervals, reducing average peak density of unphosphorylated I_{Ca}, at 0 mV, from −4.07 to −2.58 pA/pF (N=9, p=0.004; Fig. 1D). In all experiments, *I-V* protocols were applied following the single-step-pulse depolarization protocol, with at least one-minute interval between the two protocols. During this interval, I_{Ca} further decreased by about 5–10% (Fig. 1B), possibly related to slow exchange of the t-tubular space or I_{Ca} run down. To exclude the complicating factor of Ca^{2+} channel run down from data analysis, the suppressive effects of low Na^+ were generally quantified only in the first 10 to 15 sec of low Na^+ exposure. *I-V* relations in low Na^+ were often shifted by ~ −10 mV in both the apparent reversal potential and the peak inward current. The activation and availability parameters of I_{Ca}, measured with test and conditioning pulse protocols, respectively, showed no significant change (p=0.79) in activation parameter, but there was a small statistically significant shift of −3.45 mV (p=0.039) in the half-maximal voltage ($V_{0.5}$) of availability curve, with no change in the slope factor (p=0.74; Fig. 1E).

3.2. The Low Na^+ effect in PKA phosphorylated chnnels

L-type Ca^{2+} channels are regulated by PKA phosphorylation leading to their increased mean open time, open probability and influx of permeating cations [5,19–20]. To examine whether PKA-induced phosphorylation altered the low Na^+ effect, 200 μM cAMP was included in the patch pipette solutions. Peak I_{Ca} in cAMP dialyzed cells ranged between 8–25 pA/pF as compared to 2–6 pA/pF in contol solutions. Figure 2 shows that I_{Ca} decreased by 33 % within the first 15 s of solution exchange, as compared to 43±4%, measured during more protracted recordings of I-V relations (Fig. 2AB). Similar suppressive effects were seen at all voltages tested. The activation curves were once again not significantly changed, but the availability parameters showed a statistically significant −5.6 mV (p=0.005) shift in $V_{0.5}$ with no or minor change in the slope factor (p=0.98; panel 2E). These results suggest that the suppressive effects of low Na^+ were not significantly altered by the phosphorylation state of the channel.

3.4. Concentration-dependence of the low Na^+ effect

We used concentrations of Na^+ ranging from 10–145 mM to determine the concentration-dependence of the low Na^+ effect. Because the low Na^+ effect was not significantly altered by channel phosphorylation, in this set of experiments 200 μM cAMP was included the patch pipette solutions to minimize the Ca^{2+} current run down. Figure 3 shows that I_{Ca}

decreased as a function of reducing the $[Na^+]_o$ from 145 to 70 mM, but the suppressive effect below 70 mM leveled off at 33% of the current in control solutions. I_{Ca} suppression was 25%, 20% and 15% with 100, 120 and 130 mM Na^+ respectively, with an IC_{50} at 128 mM, when measured 10–15 s following reduction of Na^+ (Fig. 3A). Figure 3B–D show cumulative time course of suppression of I_{Ca} seen in experiments with 10 s exposure to solution with 50, 100 and 120 mM $[Na^+]_o$ (N=4–5). Increasing Na^+ back to control levels recovered I_{Ca} to 95% of its baseline values within 5–15 seconds.

In the experiments of Figure 3, since Cs^+ was used to replace Na^+, we tested if differential surface charge effects between the two cations were responsible for the degree of the current suppression by varying the extracellular Cs^+ concentrations from 20–100 mM while keeping the concentration of Na^+ constant at 50 mM, using sucrose to compensate for the osmotic imbalance. Figure 4 shows that changing Cs^+ concentration in the presence of 50 mM $[Na]_o$ neither altered the suppressive effect of low Na^+ on I_{Ca} (ANOVA N=4, p=0.56; panel 4C), nor did it change its voltage-dependence, or gating parameters (data not shown). Our data, therefore, do not support significant role for differential surface charge screening effects of these two monovalents.

3.5. Modulation of low Na^+ effects on I_{Ca} by different monovalent substitutions

Figure 5A–C compares *I-V* relation of I_{Ca} obtained by replacing all but 10 mM NaCl with equivalent amounts of LiCl (A), CsCl (B) and TEACl (C). Consistently, LiCl decreased I_{Ca} by only 18% (from 8.7±1.3 to 7.1±1.1 pA/pF; N=7, p=0.002) as compared to 38% suppression by Cs^+. TEA substitution produced the largest (~45%) suppression of I_{Ca} from 10.5±1.5 to 5.9±1.0 pA/pF (N=6, p=0.01; see also figure 5E). The smaller effect of substituting Li^+ may be related to its comparable size to Na^+, while TEA^+, with its larger size and hydration shell, is least likely to replace Na^+ within the outer vestibule of channel pore, and may thus produce the largest suppressive effect on I_{Ca}. Interestingly, only replacement of Na^+ with Cs^+, but not Li+ or TEA produced a small negative shift in the apparent reversal potential of I_{Ca} (compare panels A, B, & C of Fig. 5).

3.6. The low Na^+ effect on the recombinant L-type Ca^{2+} channel

In order to validate the low Na^+ suppressive effect as a property of the L-type channel protein, we examined this effect in HEK 293 cell expressing all the subunits of the L-type channel gene ($\alpha_{1C,77}$-YFP, β_1, and $\alpha_2\delta$). Figure 6A, shows *I-V* relation of I_{Ca} before and after exposure of the cell to 10 mM $[Na^+]_o$ using Cs^+ as the substituting cation for Na^+. I_{Ca} was suppressed by 20% from its control values within 10 s of the exchange of extracellular solutions (N=6, p=0.001). When Ba^{2+} was the charge carrier through the channel withdrawal of Na^+ similarly suppressed $I_{Ba..}$ Figure 6B–C shows representative traces of I_{Ba} suppression at the two concentrations of Na^+, while Figure 6D depicts the time course of I_{Ba} suppression on reducing Na^+ to 120 mM. Quantitative representation of data at the two concentrations using either sucrose or Cs^+ (N=4 and 8 respectively) is shown in Figure 6E. Maximal suppression of I_{Ca} was 23% in 10 mM Na^+ and 14% in 120 mM $[Na]_o$. These values are slightly smaller than those observed in native cardiac myocytes, but do show similar suppressive effects of low Na^+ on I_{Ca}. It is possible that the differences between native myocyte and recombinant Ca^{2+} channels are related to post translational modification such as glycosylation of the $\alpha_2\delta$ subunit [21–22].

3.7. Evaluating the Role of NCX and Localized CICR in the Low Na^+ Effect

Entry of Ca^{2+} through the L-type Ca^{2+} channel not only inactivates the channel (CDI), but also induces SR Ca^{2+} release which further contributes to CDI of the channel [23–24]. Using weakly Ca^{2+}-buffered internal solutions (2 mM EGTA), therefore we probed whether reducing the extracellular Na^+, which enhances Ca^{2+} influx on NCX, might inactive I_{Ca}

directly, or indirectly by activating Ca^{2+} release (CICR) from SR. This possibility was tested by repeating the above experiments using Ba^{2+} (known not to activate CICR, [25]) as the charge carrier through the Ca^{2+} channels. Figure 7A depicts the cumulative time course of this response at extracellular Na^+ concentrations of 10, 70, 100 and 120 mM. Similar to the observed suppressive effects of low Na^+ on I_{Ca}, Ba^{2+}-transporting channels were also suppressed in a concentration dependent manner. Somewhat larger suppressions were noted in Ba^{2+} transporting channels: 44% in 10 mM Na^+, 36% in 70 mM Na^+ and 22% in 120mM Na^+ (panel 7E). Interestingly, with Ba^+ as charge carrier, a relatively larger shift in the apparent reversal potential (~−12 mV; panel 7C) and smaller shift in the activation curve (~ −7 mV; panel 7D), were noted only when Cs^+ substituted for Na^+. The similarity of low Na^+ suppressive effects on I_{Ba} and I_{Ca} rules out significant role for involvement of NCX and CICR in the low Na^+ response.

3.8. Do longer mean open times enhance the low Na^+ suppressive effects?

In support of this idea the low Na^+ suppressive effects were larger (Fig. 7) when channel mean open times were prolonged by inhibiting CDI and CICR in Ba^{2+} transporting channels. We further probed this idea by using the Ca^{2+} channel agonist (S)-(−)-Bay K 8644, known to prolong the mean open time of the channel and to desensitize the channel to Ca^{2+} dependent inactivation [22,26–28]. Application of 1 μM Bay K 8644 increased peak I_{Ca} from an average of 10 pA/pF to 17.4 pA/pF and slowed the inactivation kinetics by 53% at 0 mV (τ=5.1±1.9 *vs.* 10.8±3.1). Figure 8A shows a decrease in I_{Ca} of approximately 30% within the first 5 s of removal of Na^+ and a maximal suppression 43% in ~15 s. Interestingly, the low Na^+ suppressive effect in Bay K 8644 containing solutions (43%) was similar to that observed when Ba^{2+} was the charge carrier through the channel (44%). Peak I_{Ca} decreased from −17.4±2.2 to −8.3±1.4 pA/pF (N=5; panel 8C). These results suggest that prolonged mean open time of the channel or removing Ca^{2+} dependent inactivation sensitizes the channel to the effects of low $[Na^+]_o$.

3.9. pH-dependence of the low Na^+ effect

Under physiological conditions, an increase in extracellular proton concentrations has the strongest suppressive effects on the Ca^{2+} channel amongst the monovalents cations. We therefore tested if the effects of low Na^+ might be influenced by acidification in a manner suggesting a common regulatory mechanism. Figure 9 compares the effect of changes in pH from 7.4 to 10, 8, and 6 in 145 (panels A,C,E) and 10 mM Na^+ (panels B,D,F) on I_{Ba} measured in HEK cells expressing the recombinant L-type Ca^{2+} channel. Changing extracellular pH from 7.4 to 8 or 10 produced proportional enhancements of the current irrespective of the Na^+ concentration (145 or 10 mM). However, at pH 6.7 there was a significant difference in the degree of suppression of I_{Ba} depending on external Na^+ concentrations (50% in 145 and 60% in 10 mM Na^+, Fig. 9G). At pH 6 the Na^+ dependent suppressive effect of protons was even more pronounced (67% in 145 and 99% in 10 mM Na^+, Fig. 9, EFG). The I-V relations in panels 9 H (145 mM Na^+) and 9 I (10 mM Na^+) show that such low pH values both reduce I_{Ba} and shift the $V_{0.5}$ of activation parameter to more positive values. The voltage-dependence of the suppression of the Ca^{2+} channel current at pH 6 suggests that near complete block of the current may be anticipated at negative potentials, in 10 mM Na^+ concentrations (Fig. 9J), but the block was mostly relieved at positive voltages, particularly in 145 mM Na^+.

4. Discussion

This study provides novel insight into regulation of I_{Ca} by external Na^+. We find that the reduction in current through the Ca^{2+} channel in Na^+-deficient solutions is: a) rapid (5–15s), reversible (Figs. 1A, 2A, 3BCD, 4A, 7A, 8A), and dose-dependent (at a range relevant to

clinical hyponatremia, 145–120 mM $[Na^+]_o$; Figs. 3, 6E, 7), b) independent of phosphorylation state of the channel (Fig. 2), c) somewhat dependent on the species of substituting monovalents ($Li^+ <. Cs^+ <$ TEA; Figs. 4, 5, 6E), the permeating divalent (Ca^{2+} *vs.* Ba^{2+}), and the cellular environment of the native myocyte *vs.* heterologously expressed channel in HEK cells (Figs. 1–5, 7, 8 *vs*. 6, 9), but d) strongly modulated by acidification and agents that enhance the mean-open-time of the channel (Bay K, and Ba^{2+}, Figs. 7 and 8).

Our results support the idea that Na^+ interacts directly with the Ca^{2+} channel. We propose that Na^+ may penetrate into the outer opening of the channel and occupy, in part, site(s) that are modulated by protons. This assessment is based on the evidence provided against direct Na^+ permeation and CDI of the channel by influx of Ca^{2+} on NCX or CICR and on our new data in conjunction with published single-channel measurements, structural information, mutation analyses, and modeling efforts [29].

4.1. The Permeation Hypothesis Revisited

The primary evidence supporting direct permeation of Na^+ through the Ca^{2+} channel was the report of a 8–13 mV negative shift in I_{Ca} reversal potential when extracellular Na^+ was reduced by 50% [4]. Later studies however, did not support this possibility because the high Ca^{2+} selectivity (1 μM) of the channel precludes penetration of Na^+ through the channels in presence of Ca^{2+} [3,12–13]. In addressing the permeation possibility, we examined the change in the apparent reversal potential as a function of the substituting monovalents and their concentrations and found that shifts occurred only when Cs^+ was substituted for Na^+ (especially if Ba^{2+} was the charge carrier), while the suppression of I_{Ca} with Li^+ or TEA^+ had no significant effects on I_{Ca} reversal potential (Fig. 5). Cs^+, however, produced no additional change in the reversal potential when substituting for $[Na^+]_o$ below 100 mM concentrations (*Cf.* Fig. 3) or when Cs^+ was used in a variable mixture with sucrose at a fixed $[Na^+]_o$ of 50 mM (*Cf.* Fig. 4). The observed shifts in reversal potential (and activation curve; Fig. 7D) may be, in part, related to estimated −5 mV liquid junction potentials for Cs^+. In short, our data do not support a correlation between the $[Na^+]_o$-induced changes in the magnitude and reversal potential of the current through the Ca^{2+} channel.

Considering the dose-response relation (Fig. 3), we note that lowering Na^+ incrementally from 145-10 mM leads to a non-linear suppression of I_{Ca}, such that decreasing the Na^+ concentrations from 145-70 mM Na^+ decreased I_{Ca} in a concentration dependent manner, while from 70 to 10 mM the current was virtually independent of $[Na^+]_o$ both in cardiomyocytes and the HEK cell expression system (Fig. 10A). Specifically, while a 25 mM reduction in Na^+ from 145-120 mM suppressed I_{Ca} in ventricular cells by 20%, a 14 fold decrease from 70 to 5 mM suppressed the current by only another 13%. In contrast, if Na^+ were permeating together with Ca^{2+} through the channel, then IC_{50} of the concentration-dependent suppression more likely would have been around 70 mM Na^+, and not the measured 128 mM. We therefore conclude that permeation cannot contribute significantly to the low Na^+-induced suppression of I_{Ca}.

4.2. Role of NCX in Ca^{2+}-dependent inactivation of I_{Ca}

The low Na^+ suppression of I_{Ca} may also be mediated by CDI of the channel, secondary to influx of Ca^{2+} on NCX [3]. In physiological solutions (145 mM Na^+) and free cytosolic Ca^{2+} of 100 nM, NCX operates primarily in the Ca^{2+} influx mode at voltages positive to −30 mV. In 10 mM Na^+ solutions, however, $E_{Na/Ca}$ would shift to highly negative voltages of about −200 mV, greatly increasing the influx of Ca^{2+} on NCX, suppressing thereby I_{Ca} *via* the CDI mechanism. To circumvent this possibility cells were dialyzed with Na^+-free solutions, which shifts $E_{Na/Ca}$ to positive potentials, counteracting the low external Na^+-

induced negative shift of $E_{Na/Ca}$ and minimizing Ca^{2+} entry on NCX. Since our results continued to show low Na^+-induced I_{Ca} suppression even in zero Na^+ dialyzed cells, we considered this mechanism improbable. This was also consistent with the findings that when Ba^{2+} was used as the charge carrier through the channel to prevent Ca^{2+} release from the SR [25], the suppressive effects of low Na^+ on the Ca^{+2} channel were not significantly altered (Fig. 7).

4.3. Mechanism of Regulation of the Ca^{2+} Channel by Extracellular Na^+

Although direct channel modulation by external Na^+ has been considered [5], little evidence exists in its support. Several experimental approaches in the present study were directed at probing such a mechanism. Though the detailed structure of the pore-forming α_1-subunit is still unknown [15], it is recognized that mutation of 4 centrally located glutamate residues (Fig. 10B; EEEE) strongly affects high-affinity Ca^{2+} binding, selectivity, threshold of activation, and pH-sensitivity of the channel [15,29–30] thereby accounting for some of the major differences between high and low threshold Ca^{2+} channels, as well as the Na^+ channel. The outer vestibule of the channel is also populated by acidic residues that may also modulate the conductance of the channel by establishing a negatively charged environment where cations can either bind to specific sites [31] or compete for the available space based on size, charge, and ability to incorporate carboxylate oxygens in their hydration shells [32].

This framework may be considered in the interpretation of our results. For instance, the efficacy of the substituting ions maybe related to their hydrated radii ($Li^+ < Cs^+ < TEA^+$), which in turn would govern their penetration into the outer reaches of the channel pore. Permeation of Na^+ to the selectivity filter is unlikely considering that monovalent conductance by the channel is abolished by μ-molar concentrations of Ca^{2+} [33]. The non-linear dose-response curves, showed no indication of saturation at $[Na^+]_o$ of 145 mM and was not significantly altered by higher (155 mM) Na^+ concentrations (Fig. 3A). In fact, irrespective of experimental condition, the effect on the Ca^{2+} channel current was in excess of cubed function of $[Na^+]_o$ (Fig. 10A, dashed curve) suggesting a high degree of cooperativity. The multiple acidic residues in channel pore may favor high-cooperativity, but considering the substantial residual conductance (~55–70% at pH 7.4 and 10 mM Na^+), it is also likely that a Na^+-dependent linear permeation process (Fig. 10A; dotted line) is partially masked by a parallel Na^+-independent permeation process. Figure 10C illustrates the combined effects of H^+ and Na^+ where the currents are all normalized relative to the value at pH 7.4 and 145 mM Na^+ (*Cf.* Fig. 9G). Plotted this way it appears, that the IC_{50} of pH-dependence of the current is nearly independent of $[Na^+]_o$ while the Na^+-dependent component of the current is nearly the same at all pH values. This may be compared to the finding that acidification reduces the single Ca^{2+}channel conductance from 140 to 45 pS [15,34]. To distinguish more clearly between the effects of Na^+ and H^+, we analyzed the *I-V* relations (Fig. 8H, I) in terms of conductance and $V_{0.5}$ of the activation parameter. The Na^+-sensitive component of the whole-cell conductance amounted to ~30 nS and was insensitive to pH compared to the remaining conductance that changed gradually in the entire range from pH 6 to 10 (Fig. 10D). Similarly, the small Na^+-dependent shift in the activation curves was independent of pH, but superimposed on a much larger pH-dependent shift at pH 6.0, which may account for the high overall pH-sensitivity of I_{Ca} in the narrower range of normal and slightly acidic conditions (Fig. 10E; *Cf.* [35]). Since mutation of the domain I and III glutamates of the EEEE locus abolishes the high-conductance state and renders the channel insensitive to pH [15], it would be of interest to test its sensitivity to Na^+ under these conditions. In summary, our results are consistent with the notion that Na^+ and H^+ penetrate into the opening of the channel where they exert parallel, but antagonistic effects on channel conductance. Ultimately these effects may involve the selectivity filter, but it is

as yet unclear whether the sensing of Na^+ and H^+ occurs at the same site. Similar considerations apply to our results testing phosphorylation (Fig. 2) and (S)-(−)Bay K 8644 (Fig. 8). Both interventions are known to enhance long openings of the Ca^{2+} channel [12,36], but the mechanism would appear to be different since (S)-(−)-Bay K 8644, and dihydropyridines in general, are thought to penetrate into the outer vestibule [37–38], but PKA-dependent phosphorylation does not appear to directly target residues within the permeation pore [39]. Therefore, our findings that (S)-(−)-Bay K 8644 (Fig. 8), but not cAMP (Fig. 2) enhance the Na^+-sensitivity of the channel are also consistent with the notion that Na^+ interacts directly with the regulatory sites within the permeation pore.

5. Pathophysiological relevance

Hyponatremia is a clinical condition that results from a decline of serum Na^+ levels below 134 mM. Duration and severity of hyponatremia is a strong predictor of clinical outcomes in many conditions including heart failure and myocardial infarction. It has long been known that patients with heart failure who also suffer from chronic hyponatremia have poor prognostic outcomes and have an increased rate of mortality [1]. Additionally patients with serum Na^+ levels below 136 mM have an increased risk of developing heart failure and mortality post myocardial infarction [2,40]. To date, no studies have mechanistically explored the link between hyponatremia and depressed cardiac contractility. Our studies here show that replacement of extracellular Na^+ by other cations or sucrose directly suppressed L-type Ca^{2+} current in a concentration dependent manner with an IC_{50} of 128 mM (Figure 3). Since suppression of I_{Ca} in low Na^+ is independent of channel phosphorylation, Ca^{2+}-induced Ca^{2+} release, activation of Ca^{2+} influx mode of NCX, and is present in recombinant channel expressed in HEK cells, it is likely that it is a direct property of the channel itself. Na^+ concentrations between 100–135 mM are concordant with serum Na^+ levels associated with symptomatic hyponatremia. Decreased Ca^{2+} conductance with decreased external Na^+ may in part explain the depressed cardiac contractility and poor outcomes encountered by patients suffering from persistent hyponatremia and heart failure especially under systemic or local acidosis commonly seen with ischemic injury.

Acknowledgments

This work was supported by NIH grants HL-16152 and 5 F32HL088855.

Abbreviations

NCX	Na^+/Ca^{2+} exchanger
CICR	Ca^{2+}-induced Ca^{2+} release
CDI	Ca^{2+}-dependent inactivation
PKA	protein kinase A
GFP	green fluorescent protein
SR	sarcoplasmic reticulum
I-V	current-voltage

References

1. Brandimarte F, Fedele F, De Luca L, Fonarow GC, Gheorghiade M. Hyponatremia in acute heart failure syndromes: a potential therapeutic target. Curr Heart Fail Rep. 2007; 4:207–213. [PubMed: 18221617]

2. Goldberg A, Hammerman H, Petcherski S, et al. Hyponatremia and long-term mortality in survivors of acute ST-elevation myocardial infarction. Arch Intern Med. 2006; 166:781–786. [PubMed: 16606816]
3. Matsuda H, Noma A. Isolation of calcium current and its sensitivity to monovalent cations in dialysed ventricular cells of guinea-pig. J Physiol. 1984; 357:553–573. [PubMed: 6096535]
4. Reuter H, Scholz H. A study of the ion selectivity and the kinetic properties of the calcium dependent slow inward current in mammalian cardiac muscle. J Physiol. 1977; 264:17–47. [PubMed: 839451]
5. McDonald TF, Pelzer S, Trautwein W, Pelzer DJ. Regulation and modulation of calcium channels in cardiac, skeletal, and smooth muscle cells. Physiol Rev. 1994; 74:365–507. [PubMed: 8171118]
6. Noma A, Yanagihara K, Irisawa H. Inward current of the rabbit sinoatrial node cell. Pflugers Arch. 1977; 372:43–51. [PubMed: 563583]
7. Bonvallet R, Rougier O. The effects of sodium removal on the two types of calcium currents in single frog atrial cells. Gen Physiol Biophys. 1991; 10:523–536. [PubMed: 1666387]
8. Mitchell MR, Powell T, Terrar DA, Twist VW. Characteristics of the second inward current in cells isolated from rat ventricular muscle. Proc R Soc Lond B Biol Sci. 1983; 219:447–469. [PubMed: 6139821]
9. Hume JR, Giles W. Ionic currents in single isolated bullfrog atrial cells. J Gen Physiol. 1983; 81:153–194. [PubMed: 6302197]
10. Nilius B, Hess P, Lansman JB, Tsien RW. A novel type of cardiac calcium channel in ventricular cells. Nature. 1985; 316:443–446. [PubMed: 2410797]
11. Campbell DL, Giles WR, Shibata EF. Ion transfer characteristics of the calcium current in bull-frog atrial myocytes. J Physiol. 1988; 403:239–266. [PubMed: 2855341]
12. Hess P, Tsien RW. Mechanism of ion permeation through calcium channels. Nature. 1984; 309:453–456. [PubMed: 6328315]
13. Almers W, McCleskey EW, Palade PT. A non-selective cation conductance in frog muscle membrane blocked by micromolar external calcium ions. J Physiol. 1984; 353:565–583. [PubMed: 6090645]
14. Santarelli VP, Eastwood AL, Dougherty DA, Ahern CA, Horn R. Calcium block of single sodium channels: role of a pore-lining aromatic residue. Biophys J. 2007; 93:2341–2349. [PubMed: 17545248]
15. Chen XH, Bezprozvanny I, Tsien RW. Molecular basis of proton block of L-type Ca2+ channels. J Gen Physiol. 1996; 108:363–374. [PubMed: 8923262]
16. Pietrobon D, Prod'hom B, Hess P. Interactions of protons with single open L-type calcium channels. pH dependence of proton-induced current fluctuations with Cs+, K+, and Na+ as permeant ions. J Gen Physiol. 1989; 94:1–21. [PubMed: 2553855]
17. Knollmann BC, Knollmann-Ritschel BE, Weissman NJ, Jones LR, Morad M. Remodelling of ionic currents in hypertrophied and failing hearts of transgenic mice overexpressing calsequestrin. J Physiol. 2000; 525(Pt 2):483–498. [PubMed: 10835049]
18. Belmonte S, Morad M. 'Pressure-flow'-triggered intracellular Ca2+ transients in rat cardiac myocytes: possible mechanisms and role of mitochondria. J Physiol. 2008; 586:1379–1397. [PubMed: 18187469]
19. Reuter H, Scholz H. The regulation of the calcium conductance of cardiac muscle by adrenaline. J Physiol. 1977; 264:49–62. [PubMed: 839456]
20. Catterall WA. Structure and regulation of voltage-gated Ca2+ channels. Annu Rev Cell Dev Biol. 2000; 16:521–555. [PubMed: 11031246]
21. Douglas L, Davies A, Wratten J, Dolphin AC. Do voltage-gated calcium channel alpha2delta subunits require proteolytic processing into alpha2 and delta to be functional? Biochem Soc Trans. 2006; 34:894–898. [PubMed: 17052222]
22. Canti C, Nieto-Rostro M, Foucault I, et al. The metal-ion-dependent adhesion site in the Von Willebrand factor-A domain of alpha2delta subunits is key to trafficking voltage-gated Ca2+ channels. Proc Natl Acad Sci U S A. 2005; 102:11230–11235. [PubMed: 16061813]
23. Sham JS, Cleemann L, Morad M. Functional coupling of Ca2+ channels and ryanodine receptors in cardiac myocytes. Proc Natl Acad Sci U S A. 1995; 92:121–125. [PubMed: 7816800]

24. Adachi-Akahane S, Cleemann L, Morad M. Cross-signaling between L-type Ca2+ channels and ryanodine receptors in rat ventricular myocytes. J Gen Physiol. 1996; 108:435–454. [PubMed: 8923268]
25. Nabauer M, Callewaert G, Cleemann L, Morad M. Regulation of calcium release is gated by calcium current, not gating charge, in cardiac myocytes. Science. 1989; 244:800–803. [PubMed: 2543067]
26. Mentrard D, Vassort G, Fischmeister R. Calcium-mediated inactivation of the calcium conductance in cesium-loaded frog heart cells. J Gen Physiol. 1984; 83:105–131. [PubMed: 6319542]
27. Hess P, Lansman JB, Tsien RW. Calcium channel selectivity for divalent and monovalent cations. Voltage and concentration dependence of single channel current in ventricular heart cells. J Gen Physiol. 1986; 88:293–319. [PubMed: 2428919]
28. Adachi-Akahane S, Cleemann L, Morad M. BAY K 8644 modifies Ca2+ cross signaling between DHP and ryanodine receptors in rat ventricular myocytes. Am J Physiol. 1999; 276:H1178–1189. [PubMed: 10199841]
29. Sather WA, McCleskey EW. Permeation and selectivity in calcium channels. Annu Rev Physiol. 2003; 65:133–159. [PubMed: 12471162]
30. Talavera K, Staes M, Janssens A, et al. Aspartate residues of the Glu-Glu-Asp-Asp (EEDD) pore locus control selectivity and permeation of the T-type Ca(2+) channel alpha(1G). J Biol Chem. 2001; 276:45628–45635. [PubMed: 11526105]
31. Feng ZP, Hamid J, Doering C, et al. Amino acid residues outside of the pore region contribute to N-type calcium channel permeation. J Biol Chem. 2001; 276:5726–5730. [PubMed: 11120735]
32. Nonner W, Eisenberg B. Ion permeation and glutamate residues linked by Poisson-Nernst-Planck theory in L-type calcium channels. Biophys J. 1998; 75:1287–1305. [PubMed: 9726931]
33. Yang J, Ellinor PT, Sather WA, Zhang JF, Tsien RW. Molecular determinants of Ca2+ selectivity and ion permeation in L-type Ca2+ channels. Nature. 1993; 366:158–161. [PubMed: 8232554]
34. Prod'hom B, Pietrobon D, Hess P. Interactions of protons with single open L-type calcium channels. Location of protonation site and dependence of proton-induced current fluctuations on concentration and species of permeant ion. J Gen Physiol. 1989; 94:23–42. [PubMed: 2553858]
35. Delisle BP, Satin J. pH modification of human T-type calcium channel gating. Biophys J. 2000; 78:1895–1905. [PubMed: 10733969]
36. Ochi R. Single-channel mechanism of beta-adrenergic enhancement of cardiac L-type calcium current. Jpn J Physiol. 1993; 43:571–584. [PubMed: 7908347]
37. Kwan YW, Bangalore R, Lakitsh M, Glossmann H, Kass RS. Inhibition of cardiac L-type calcium channels by quaternary amlodipine: implications for pharmacokinetics and access to dihydropyridine binding site. J Mol Cell Cardiol. 1995; 27:253–262. [PubMed: 7760349]
38. Tikhonov DB, Zhorov BS. Structural model for dihydropyridine binding to L-type calcium channels. J Biol Chem. 2009; 284:19006–19017. [PubMed: 19416978]
39. Erxleben C, Gomez-Alegria C, Darden T, Mori Y, Birnbaumer L, Armstrong DL. Modulation of cardiac Ca(V)1.2 channels by dihydropyridine and phosphatase inhibitor requires Ser-1142 in the domain III pore loop. Proc Natl Acad Sci U S A. 2003; 100:2929–2934. [PubMed: 12601159]
40. Singla I, Zahid M, Good CB, Macioce A, Sonel AF. Effect of hyponatremia (<135 mEq/L) on outcome in patients with non-ST-elevation acute coronary syndrome. Am J Cardiol. 2007; 100:406–408. [PubMed: 17659918]

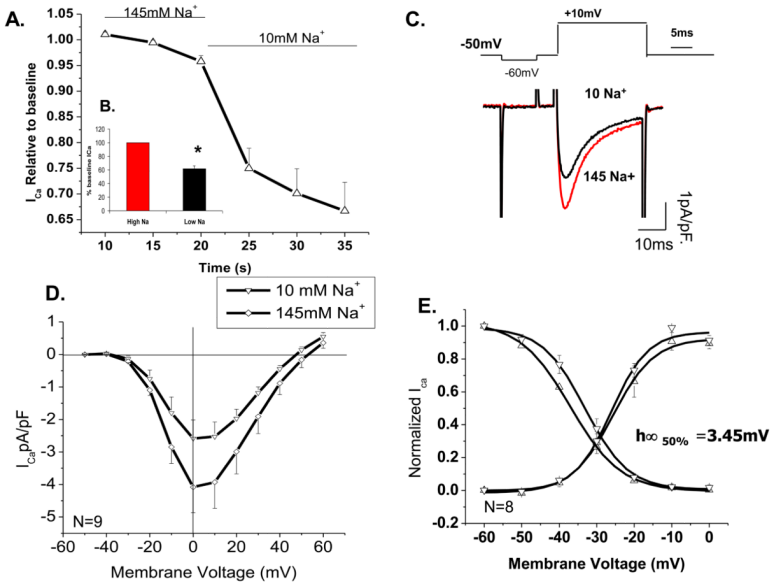

Figure 1. Reducing extracellular [Na^+] leads to suppression of baseline unphosphorylated I_{Ca}

A) Time course of peak I_{Ca} suppression under rapid fluid exchange to low (10mM) extracellular [Na^+]. Currents were recorded under a single step depolarization to +10 mV from holding potential of −50 mV. B) Quantitative representation of peak I_{Ca} suppression in low $[Na^+]_o$ solutions. C) Representative peak traces from high and low extracellular [Na^+] in the same cell. D) *I-V*-relation of I_{Ca} in 145 (◇) and 10 mM (▽) extracellular [Na^+] (N=9, p=0.004). E) Corresponding activation and availability plots at 145 mM Na^+ (▽) and 10 mM Na^+ (△) (N=8). For measurements of availability, the membrane was held for 500 ms at a conditioning potential ranging from −80 to +30 mV and followed by a depolarizing test pulse to +10mV.

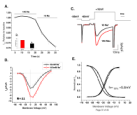

Figure 2. Reducing extracellular [Na^+] leads to suppression of phosphorylated I_{Ca}

A) Time course of peak I_{Ca} suppression under rapid fluid exchange to low (10 mM) extracellular [Na^+]. B) Quantitative representation of peak I_{Ca} suppression in low $[Na^+]_o$ solutions. C) Representative peak traces from high and low extracellular [Na^+] in the same cell. D) *I-V*-relation of I_{Ca} in 145mM (◇) and 10mM (▽) extracellular [Na^+] (N=11, p=0.007). E) Corresponding activation/availability plots measured with 145 mM (▽) or 10 mM $[Na^+]_o$ (△; N=9).

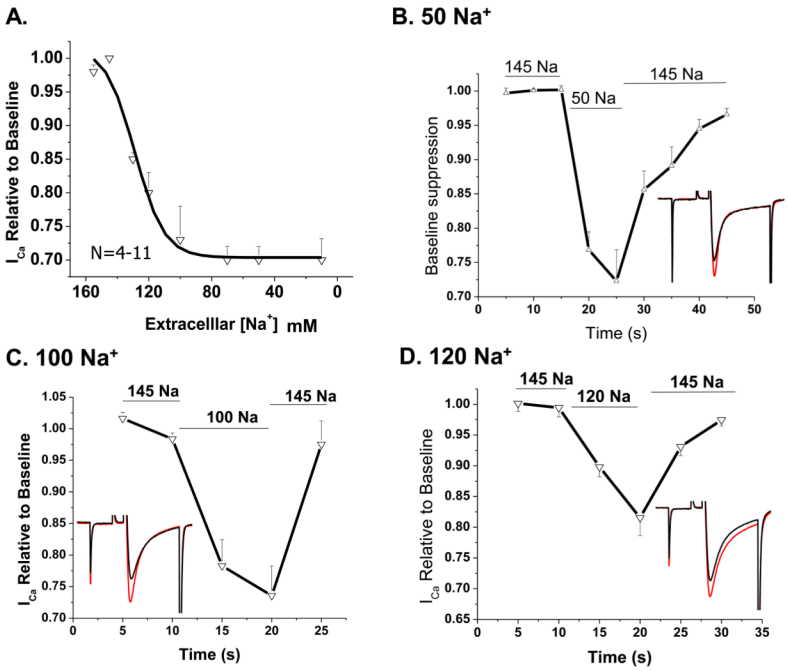

Figure 3. I_{Ca} suppression in low extracellular [Na^+] is concentration dependent at $[Na^+]_o$ above 100 mM

A) Concentration-dependence of I_{Ca} suppression in various extracellular Na^+ concentrations ranging from 145 to 10 mM (N=4–11, $p<0.01$ at all points). B–D) Time course of I_{Ca} suppression in extracellular solutions containing 50, 100, 120 mM NaCl respectively. Extracellular Na^+ was replaced by equivalent amount of Cs^+.

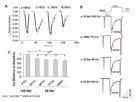

Figure 4. Extracellular Cs^+ concentration does not affect the degree of I_{Ca} suppression by removal of extracellular Na^+

A) Cumulative timeline of I_{Ca} suppression in 50 mM extracellular Na^+ using varying concentrations of CsCl 100 (a), 70 (b), 50 (c) and 20 mM (d) as the substituting cation and with sucrose added to maintain constant osmolarity. B) Representative currents from a single myocyte exposed to 50 mM external Na^+ along with varying external CsCl (20–100mM, a–d). C) Quantitative representation of A in 4 cells. $P<0.005$ compared to control, $P=0.56$ between the various concentrations using a one way ANOVA.

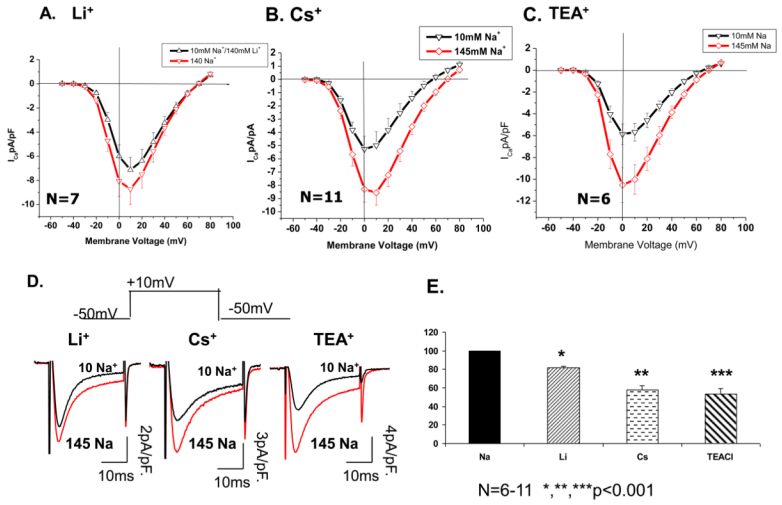

Figure 5. I_{Ca} suppression depends on the ionic properties of the extracellular monovalent cation

A–C) *I-V* relation of I_{Ca} in external solutions containing 145mM (◇) and 10 mM (▽) NaCl using 140 mM of LiCl, CsCl or TEACl to replace the remaining NaCl. D) Representative traces of I_{Ca} suppression in 10 mM Na^+ replacing the extracellular cation with Li^+, Cs^+ and TEA^+. E) Quantitative representation of relative peak current suppression from baseline when extracellular monovalents were varied between Na^+, Li^+, Cs^+ and TEA^+ in 10 mM Na^+ (N=6–15, $p<0.01$ for all three conditions).

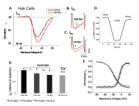

Figure 6. Low extracellular Na^+ concentration leads to I_{Ca} suppression in HEK 293 cells expressing recombinant Ca^{2+} channel

A) Current-voltage relationship of I_{Ca} in 145mM (◇) and 10mM (▽) $[Na]_o$ in HEK 293 cells expressing $\alpha_{1c,77}$, β1, $\alpha_2\delta$ subunits of the L-type Ca^{2+} channel (N=6). B–C) Representative traces from the same cell after reduction of $[Na]_o$ to 120 mM (B) and 10 mM $[Na]_o$ (C) with equi-osmolar substitution of remaining NaCl with sucrose. D) Representative time course of suppression in 120 mM external Na^+. E) quantitative representation of I_{Ba} suppression in two concentrations of 120 mM and 10 mM $[Na^+]_o$ comparing substitution with both Cs^+ and sucrose (N=5–6, $p<0.004$ for all three conditions). F) Activation and availability curves of the L-type Ca^{2+} channel in presence of 145 (◇) and 10 mM $[Na]_o$ (△) using Cs^+ as the substituting cation.

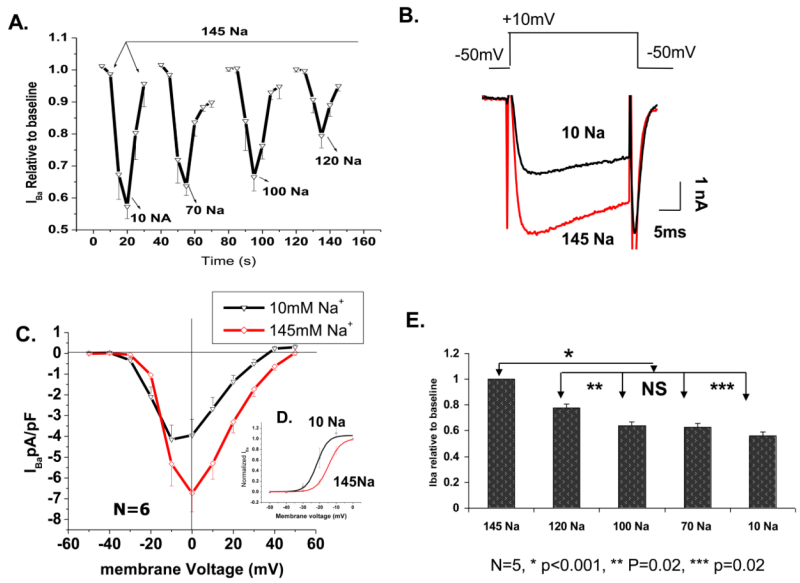

Figure 7. Reducing extracellular Na^+ leads to L-type I_{Ba} suppression in a similar fashion as I_{Ca}

A) Cumulative time course of suppression in four external NaCl concentrations (mM) of 10 (a), 70 (b), 100 (c) and 120 (d) (N=5 at each concentration). The duration of each response is depicted on the time-axis. The arrow points to control and washout and the valleys represent peak amplitude suppression at the given Na^+ concentration. B) representative Ba^{2+} current trace from a single myocyte exposed to 145 and 10 mM NaCl. C) *I-V* relation of I_{Ba} in 145mM (◇) and 10 mM (▽) NaCl extracellular solutions (N=6). D) Activation curve of I_{Ba} in high (◇) and low (△) extracellular Na^+. E) Quantitative representation of (A).

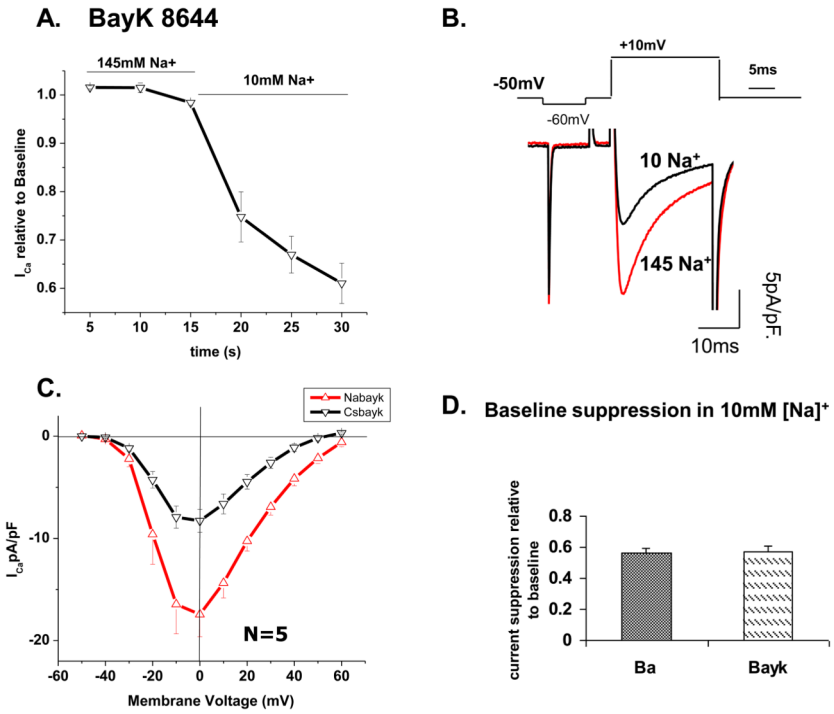

Figure 8. I_{Ca} suppression in low Na^+ is more pronounced when channels remain open with (S)-(−)-Bay K 8644

A) Time course of I_{Ca} suppression in 10 mM extracellular Na^+. Solutions were exchanged at 15 sec time point. B) Representative current trace from a cardiomyocyte incubated in 1 μM (S)-(−) Bay K 8644 before and after solution exchange to 10 mM $[Na^+]_o$. C) *I-V* relation of current suppression in high and low Na^+ extracellular solutions containing 1 μM Bay K 8644. D) Quantitative comparison of I_{Ca} (in Bay K 8644) with I_{Ba} suppression in 10 mM extracellular Na^+.

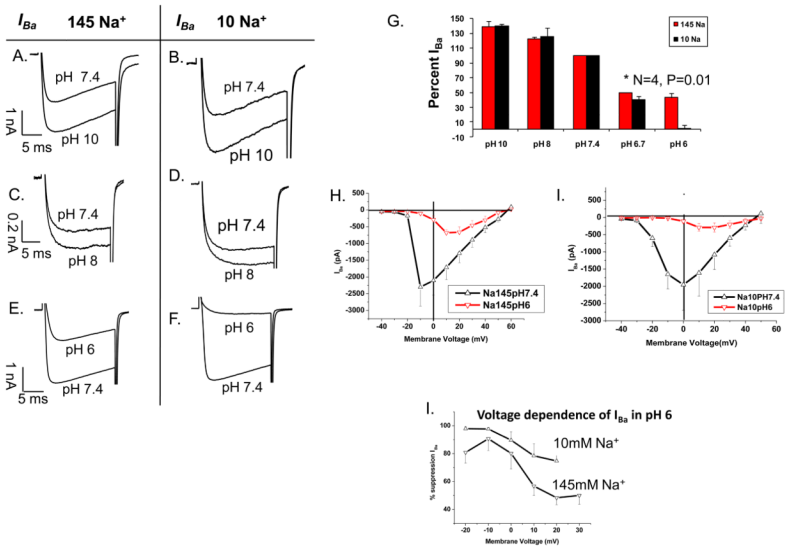

Figure 9. The effect of low extracellular [Na^+] on pH sensitivity of I_{Ba}

Panels A–F show Ba^{2+} current traces measured in the presence of 145 (A, C, E) and 10 mM (B, D, F) extracellular Na^+ in individual cells where the response to low Na^+ at pH 7.4 was compared that at either pH 10 (A–B), 8 (C–D), or 6 (E–F) G) Percent I_{Ba} compared to the current magnitude at pH 7.4 in response to varying extracellular pH values. H) *I-V* relation of I_{Ba} in 145mM external Na^+ and pH 7.4 (△) or pH 6.0 (▽) (N=4). I) *I-V* relation of I_{Ba} in 10 mM external Na^+ and pH 7.4 (△) or pH 6.0 (▽) (N=4). L) Voltage-dependence of I_{Ba} suppression in pH 6 and high or low external Na^+ (N=3–4).

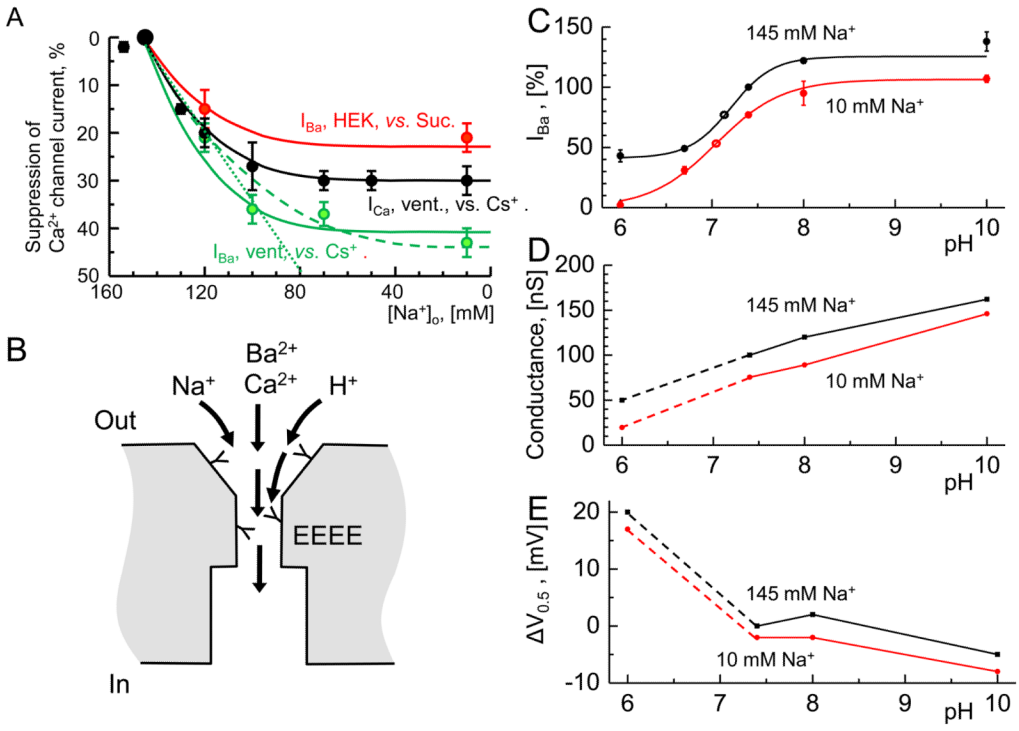

Figure 10. Summary and analysis of the suppression of the Ca^{2+} channel by low Na^+ and pH

A) Dose-response of $[Na^+]_o$ *vs.*: I_{Ca} measured with Cs^+ substitution in ventricular cells (black trace and symbols, *cf.* Fig. 3A), I_{Ba} measured with sucrose substitution in the HEK cell expression system (red, *cf.* Fig. 6E), and I_{Ba} measured with Cs^+ substitution in ventricular (green, *cf.*Fig. 7E). Solid curves are proportional to each other while the green dashed and dotted curves are cubic and linear in $[Na^+]_o$, respectively. B) Model suggesting different degrees of penetration of cations into (Na^+, H^+) and through (Ca^{2+}, Ba^{2+}) the Ca^{2+} channel where carboxylates (Y) may provide a negatively charged environment with binding sites both within the selectivity filter (EEEE locus) and in the outer vestibule. C) Combined effects of $[Na^+]_o$ and pH on I_{Ba} based on Fig. 9G, but scaled to show the average response to low Na^+ at pH 7.4. The data at different pH values were approximated with curves based on the logistic equation ($A + B/(1+([H^+]/K_D)^n)$) showing no significant change to the effective binding constant in at 145 (black, circle, K_D = 69±12 nM) *vs.* 10 mM $[Na^+]_o$ (red, circle, K_D = 90±8 nM). D) Conductance of the Ca^{2+} channel at different $[Na^+]_o$ and pH measured from the linear segment of *I-V* relations (~10–50 mV, *cf.* Fig. 9HI). E) pH- and Na^+-induced shifts in $V_{0.5}$ of activation relative to $V_{0.5}$ at pH 7.4 and 145 mM $[Na^+]_o$ (*Cf.* Fig. 9H,I).